PROCEEDINGS OF SCIENCE

New measurement of radiative decays at the NA62 experiment at CERN: $K_{e3\gamma}$

Cristina Biino[1,*]

INFN, via P. Giuria 1, Torino, Italy

E-mail: cristina.biino@to.infn.it

The NA62 experiment at CERN reports new results from studies of radiative kaon decays $K^+ \to \pi^0 e^+ \nu\gamma$ ($Ke3\gamma$), using a data sample collected in 2017-2018. The sample comprises O(100k) $Ke3\gamma$ candidates with sub-percent background contaminations. Preliminary results including the most precise measurement of the $Ke3\gamma$ branching ratios and the T-asymmetry measurement in the $Ke3\gamma$ decay, are presented.

7th Symposium on Prospects in the Physics of Discrete Symmetries (DISCRETE 2020-2021)
29th November - 3rd December 2021
Bergen, Norway

[1]for the NA62 Collaboration:
A. Akmete, R. Aliberti, F. Ambrosino, R. Ammendola, B. Angelucci, A. Antonelli, G. Anzivino, R. Arcidiacono, T. Bache, A. Baeva, D. Baigarashev, L. Bandiera, M. Barbanera, J. Bernhard, A. Biagioni, L. Bician, C. Biino, A. Bizzeti, T. Blazek, B. Bloch-Devaux, P. Boboc, V. Bonaiuto, M. Boretto, M. Bragadireanu, A. Briano Olvera, D. Britton, F. Brizioli, M.B. Brunetti, D. Bryman, F. Bucci, T. Capussela, J. Carmignani, A. Ceccucci, P. Cenci, V. Cerny, C. Cerri, B. Checcucci, A. Conovaloff, P. Cooper, E. Cortina Gil, M. Corvino, F. Costantini, A. Cotta Ramusino, D. Coward, P. Cretaro, G. Dgostini, J. Dainton, P. Dalpiaz, H. Danielsson, M. Drrico, N. De Simone, D. Di Filippo, L. Di Lella, N. Doble, B. Dobrich, F. Duval, V. Duk, D. Emelyanov, J. Engelfried, T. Enik, N. Estrada-Tristan, V. Falaleev, R. Fantechi, V. Fascianelli, L. Federici, S. Fedotov, A. Filippi, R. Fiorenza, M. Fiorini, O. Frezza, J. Fry, J. Fu, A. Fucci, L. Fulton, E. Gamberini, L. Gatignon, G. Georgiev, S. Ghinescu, A. Gianoli, M. Giorgi, S. Giudici, F. Gonnella, K. Gorshanov, E. Goudzovski, C. Graham, R. Guida, E. Gushchin, F. Hahn, H. Heath, J. Henshaw, Z. Hives, E.B. Holzer, T. Husek, O. Hutanu, D. Hutchcroft, L. Iacobuzio, E. Iacopini, E. Imbergamo, B. Jenninger, J. Jerhot, R.W. Jones, K. Kampf, V. Kekelidze, D. Kereibay, S. Kholodenko, G. Khoriauli, A. Khotyantsev, A. Kleimenova, A. Korotkova, M. Koval, V. Kozhuharov, Z. Kucerova, Y. Kudenko, J. Kunze, V. Kurochka, V. Kurshetsov, G. Lanfranchi, G. Lamanna, E. Lari, G. Latino, P. Laycock, C. Lazzeroni, M. Lenti, G. Lehmann Miotto, E. Leonardi, P. Lichard, L. Litov, P. Lo Chiatto, R. Lollini, D. Lomidze, A. Lonardo, P. Lubrano, M. Lupi, N. Lurkin, D. Madigozhin, I. Mannelli, A. Mapelli, F. Marchetto, R. Marchevski, S. Martellotti, P. Massarotti, K. Massri, E. Maurice, A. Mazzolari, M. Medvedeva, A. Mefodev, E. Menichetti, E. Migliore, E. Minucci, M. Mirra, M. Misheva, N. Molokanova, M. Moulson, S. Movchan, M. Napolitano, I. Neri, F. Newson, A. Norton, M. Noy, T. Numao, V. Obraztsov, A. Okhotnikov, A. Ostankov, S. Padolski, R. Page, V. Palladino, I. Panichi, A. Parenti, C. Parkinson, E. Pedreschi, M. Pepe, M. Perrin-Terrin, L. Peruzzo, P. Petrov, Y. Petrov, F. Petrucci, R. Piandani, M. Piccini, J. Pinzino, I. Polenkevich, L. Pontisso, Yu. Potrebenikov, D. Protopopescu, M. Raggi, M. Reyes Santos, M. Romagnoni, A. Romano, P. Rubin, G. Ruggiero, V. Ryjov, A. Sadovsky, A. Salamon, C. Santoni, G. Saracino, F. Sargeni, S. Schuchmann, V. Semenov, A. Sergi, A. Shaikhiev, S. Shkarovskiy, M. Soldani, D. Soldi, M. Sozzi, T. Spadaro, F. Spinella, A. Sturgess, V. Sugonyaev, J. Swallow, A. Sytov, G. Tinti, A. Tomczak, S. Trilov, M. Turisini, P. Valente, B. Velghe, S. Venditti, P. Vicini, R. Volpe, M. Vormstein, H.Wahl, R.Wanke, V.Wong, B. Wrona, O. Yushchenko, M. Zamkovsky, A. Zinchenko.

*Speaker

PoS(DISCRETE2020-2021)055

1. Introduction

The $K^+ \to \pi^0 e^+ \nu\gamma$ ($Ke3\gamma$) decay is described in the framework of Standard Model Chiral Perturbation theory (ChPT), with calculations of the branching ratio (BR) up to perturbation order $O(p^6)$ [1, 2, 3] . The main processes are the Inner Bremsstrahlung (IB) and Direct Emission (DE), as shown in the diagrams of Fig. 1, and their interference (INT). IB is the dominant process and the BR is strongly divergent when the photon energy E_γ or the angle $\theta_{e,\gamma}$ between the photon and the positron (in the kaon rest frame) tends to zero.

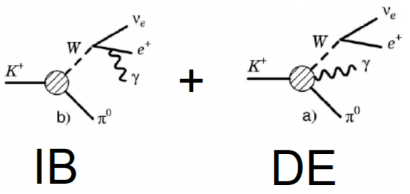

Figure 1: $K^+ \to \pi^0 e^+ \nu\gamma$ decay's diagrams: Inner Bremsstrahlung (left side), Direct Emission (right side).

DE represents about 1% of the total amplitude. The error on the DE amplitude is dominated by unknown radiative corrections and higher-order chiral corrections. R_j is defined as the ratio of the branching fraction of $K^+ \to \pi^0 e^+ \nu\gamma$ and the normalization decay $K^+ \to \pi^0 e^+ \nu$ ($Ke3$) where the j index refers to the 3 kinematic cuts, commonly used in literature and given in Table 1.

The 3 kinematic cuts (in the kaon rest frame) represent restrictions on the phase space in terms of the radiative photon energy E_γ and the angle $\theta_{e,\gamma}$. In Table 1 the current theoretical expectations and experimental results are reported.

Table 1: Status of current theoretical expectations, $O(p^6)$ ChPT calculations [1, 2, 3], and experimental results from the ISTRA+ and OKA experiments [4, 5].

	E_γ cut	$\theta_{e,\gamma} cut$	$O(p^6)$ ChPT	ISTRA+	OKA
$R_1(\times 10^2)$	$E_\gamma > 10$ MeV	$\theta_{e,\gamma} > 10°$	1.804 ± 0.021	1.81 ± 0.003 ± 0.07	1.990 ± 0.017 ± 0.021
$R_2(\times 10^2)$	$E_\gamma > 30$ MeV	$\theta_{e,\gamma} > 20°$	0.640 ± 0.008	0.63 ± 0.02 ± 0.03	0.587 ± 0.010 ± 0.015
$R_3(\times 10^2)$	$E_\gamma > 10$ MeV	$0.6 < cos\theta_{e,\gamma} < 0.9$	0.559 ± 0.006	0.47 ± 0.02 ± 0.03	0.532 ± 0.010 ± 0.012

The most recent theoretical prediction provides a result only for R_2: $(0.56 \pm 0.02)10^{-2}$ [6]. We have converted this to the normalized branching ratio for comparison with the rest of the literature. The difference from previous calculations is not negligible.

The main theoretical interest in the $K^+ \to \pi^0 e^+ \nu\gamma$ decay process is that it is possible to define, in the kaon rest frame, a T-odd variable $\xi = \overrightarrow{p_\gamma} \cdot (\overrightarrow{p_e} \times \overrightarrow{p_\pi})/m_K^3$ that allows a direct measurement of any T-violation effects, by measuring the asymmetry variable A_ξ, defined as $A_\xi = (N^+ - N^-)/(N^+ + N^-)$, where N^+ (N^-) is the number of events with positive (negative) value of ξ.

The value of A_ξ is not expected to depend strongly on the experimental cuts on E_γ and $\theta_{e,\gamma}$ and, in principle, a non-zero value for A_ξ is an indication of T-violation.

With the large data sample collected by the NA62 experiment, it is possible to improve the experimental precision for both the branching ratio and the T-asymmetry measurements.

2. The NA62 experiment

The NA62 experiment is located at the CERN SPS and operates with a (74 ± 1.4) GeV/c hadron beam (the kaon component is 6%). A detailed description of the NA62 detector and beamline can be found in [7]. The beam enters a 114 m long cylindrical vacuum tank defining the fiducial decay region. The incoming K^+ are identified by a differential Cherenkov counter (KTAG) with $\sigma = 70$ ps time resolution and their momenta are measured by a three-station silicon pixel beam-spectrometer (GTK). The positron track and momentum is reconstructed in the magnetic spectrometer (STRAW), located inside the vacuum tank. A Ring Image Cherenkov detector (RICH) provides $\pi/\mu/e$ identification. The $\pi^0 \to \gamma\gamma$ decay is identified by selecting two gammas in the liquid Krypton electromagnetic calorimeter (LKr) and applying kinematic conditions to the gamma pair invariant mass. The radiative γ is identified by selecting an in-time additional isolated cluster in the LKr. An anticoincidence between the position of a radiative γ and a track projected to the LKr plane rejects $K^+ \to \pi^0 e^+ \nu$ with a γ emitted by e^+ bremsstrahlung.

3. The NA62 measurement strategy and data selection

$$R_j = \frac{BR(K_{e3\gamma\, j})}{BR(K_{e3})} = \frac{(N^{obs}_{Ke3\gamma\, j} - N^{bkg}_{Ke3\gamma\, j})}{(N^{obs}_{Ke3} - N^{bkg}_{Ke3})} \cdot \frac{A_{Ke3}}{A_{Ke3\gamma\, j}} \cdot \frac{\epsilon^{trig}_{Ke3}}{\epsilon^{trig}_{Ke3\gamma\, j}}$$

The normalized branching ratio R_j is determined by the equation above, where $N^{obs}_{Ke3\gamma}$ (N^{obs}_{Ke3}) is the number of observed events with the signal (normalization) selection; $N^{bkg}_{Ke3\gamma}$ (N^{bkg}_{Ke3}) is the number of expected background events in the signal (normalization) selection (background estimation is performed using both data and MC simulations); $A_{Ke3\gamma}$ (A_{Ke3}) is the acceptance of the signal (normalization) selection measured with GEANT4 MC simulation with gamma overlay; $\epsilon^{trig}_{Ke3\gamma}$ (ϵ^{trig}_{Ke3}) is the trigger efficiency for the signal (normalization) selection, measured with data and is almost equal for signal and normalization (measured to be within per mill precision) since trigger conditions refer to the presence of the e^+ only. The signal $K^+ \to \pi^0 e^+ \nu\gamma$ ($Ke3\gamma$) and the normalization $K^+ \to \pi^0 e^+ \nu$ ($Ke3$) share most of the selection criteria (except for the radiative photon), implying a first order cancellation of systematics effects. The Poissonian statistical uncertainty in $N^{obs}_{Ke3\gamma_j}$ and N^{obs}_{Ke3} is propagated as statistical uncertainty in the R_j measurement, all other uncertainties are considered as systematic.

The kinematic selection is based on the missing mass (neutrino) both for signal and normalization channels where $\overrightarrow{p_{particle}}$ are the four-momenta of the reconstructed particles:

$$m^2_{miss}(K_{e3\gamma}) = (\overrightarrow{p_K} - \overrightarrow{p_e} - \overrightarrow{p_\pi} - \overrightarrow{p_\gamma})^2 \quad ; \quad m^2_{miss}(K_{e3)} = (\overrightarrow{p_K} - \overrightarrow{p_e} - \overrightarrow{p_\pi})^2$$

The kinematic signal region is defined for $|m^2_{miss}(Ke3\gamma)| < 11000\ MeV^2/c^4$ and must be compatible with 0 (neutrino squared mass) within the experimental resolution, while $m^2_{miss}(Ke3) > 5000\ MeV^2/c^4$ must be larger than 0 due to the presence of the radiative photon. On the other hand, in order to have a symmetry between the two selections, the signal and normalization regions are defined by requiring $|m^2_{miss}(Ke3\gamma)| < 11000\ MeV^2/c^4$. E_γ and $\theta_{e,\gamma}$ cuts are applied after the event selection (R_1, R_2, R_3 samples).

In Fig. 2 the main background contribution to the selected $K^+ \to \pi^0 e^+ \nu\gamma$ (signal) sample is represented by $K^+ \to \pi^0 e^+ \nu$ events with one more cluster coming from accidental (pile-up) activity in the LKr that mimics the radiative photon (so-called accidental background). The $K^+ \to \pi^0 e^+ \nu$ events can also be replaced by $K^+ \to \pi^0 \pi^+$ events with the misidentification of the charged pion. The background is evaluated with out-of-time side-bands in dedicated studies. The cut $m^2_{miss}(Ke3) > 5000\ MeV^2/c^4$ is very powerful against this category of events.

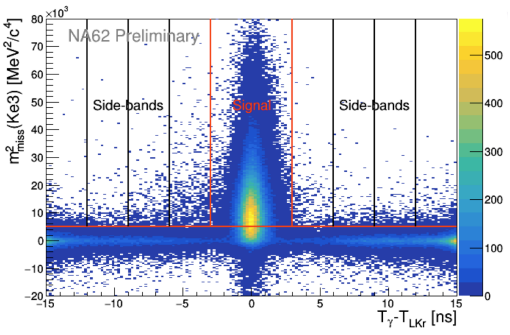

Figure 2: Reconstructed $m^2_{miss}(Ke3)$ as a function of the difference between the radiative photon cluster time T and the average time of e^+ and π^0 clusters T_{LKr}, in the $K^+ \to \pi^0 e^+ \nu\gamma$ selection. The missing mass cut is shown (red horizontal line) together with the time windows used for the radiative photon selection (±3 ns, in red) and the side-bands (in black) used for the estimation and validation of the accidental background.

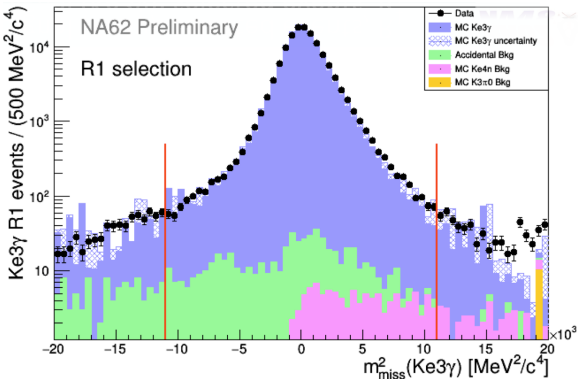

Figure 3: $m^2_{miss}(Ke3\gamma)$ for the selected $K^+ \to \pi^0 e^+ \nu\gamma$ events (in range R_1) in data (points), compared with the expected signal and all the background sources (histograms). The range 11000 MeV^2/c^4 (red lines) corresponds to the cut applied in the selection (130 K events, $B/S \simeq 0.5\%$).

The distribution of $m^2_{miss}(Ke3\gamma)$ for the R_1 events selection is shown in Fig. 3, comparing the data with the signal from MC simulation and all the background sources (all from MC, except for the accidentals extracted from data).

4. The NA62 preliminary results

In Table 2 are given the number of observed events for each kinematic cut selection and Table 3 presents a summary of all the estimated background contributions.

Table 2: Number of observed events and acceptance measurements for each kinematic cut selection. The acceptance uncertainties are limited by the MC sample statistics.

Selection	N^{obs}	Acceptance
$Ke3(norm)$	66.378×10^6	3.839 ± 0.002
$Ke3\gamma(R_1)$	129.6×10^3	0.443 ± 0.001
$Ke3\gamma(R_2)$	53.6×10^3	0.513 ± 0.002
$Ke3\gamma(R_3)$	39.1×10^3	0.431 ± 0.002

The preliminary results of the measurements of the $K^+ \to \pi^0 e^+ \nu\gamma$ branching ratio normalized to $K^+ \to \pi^0 e^+ \nu$ are reported in Table 4, compared to the state of the art.

Table 3: A summary estimate of the background contributions to the signal selection, together with the background over signal ratio (B/S), for each range of kinematic cut selection. The small values of B/S lead to a small uncertainty on the BR measurement and R_j error budget coming from the background knowledge.

Bkg source	R_1	R_2	R_3
Accidentals	$(4.9 \pm 0.2 \pm 1.3) \cdot 10^2$	$(2.3 \pm 0.2 \pm 0.3) \cdot 10^2$	$(1.1 \pm 0.1 \pm 0.5) \cdot 10^2$
$K^+ \to \pi^0\pi^0 e^+\nu$	$(1.1 \pm 1.1) \cdot 10^2$	$(1.1 \pm 1.1) \cdot 10^2$	$0.07 \pm 0.07) \cdot 10^2$
$K^+ \to \pi^+\pi^0\pi^0$	<20	<20	<20
$K^+ \to \pi^+\pi^0\gamma$	<2	<2	<2
Total	$(5.9 \pm 1.7) \cdot 10^2$	$(3.4 \pm 1.1) \cdot 10^2$	$01.1 \pm 0.6) \cdot 10^2$
B/S	0.46‰	0.64 ‰	0.29‰

Table 4: NA62 preliminary results compared to current theoretical calculations [1, 2, 3], and experimental results from ISTRA+ and OKA [4, 5].

	$O(p^6)$ ChPT	ISTRA+	OKA	NA62 preliminary
$R_1(\times 10^2)$	1.804 ± 0.021	$1.81 \pm 0.003 \pm 0.07$	$1.990 \pm 0.017 \pm 0.021$	$1.684 \pm 0.005 \pm 0.010$
$R_2(\times 10^2)$	0.640 ± 0.008	$0.63 \pm 0.02 \pm 0.03$	$0.587 \pm 0.010 \pm 0.015$	$0.599 \pm 0.003 \pm 0.005$
$R_3(\times 10^2)$	0.559 ± 0.006	$0.47 \pm 0.02 \pm 0.03$	$0.532 \pm 0.010 \pm 0.012$	$0.523 \pm 0.003 \pm 0.003$

The total systematic uncertainty is larger than the statistical one by up to a factor of 2. The R_j measurement relative precision is less than 1‰. NA62 results show an improved precision with respect to previous results by a factor between 2 and 3.6. The discrepancy with the theoretical prediction is of 6-7 ‰ in all three measurements. The NA62 result for R_2 is half way between the two latest theoretical predictions: Theor(R_2)=(0.640 ± 0.008)‰ [3] and Theor(R_2)=(0.56 ± 0.02)‰ [6]. Many extra analysis checks have been done that will be presented in detail in the paper under preparation. The stability of the branching fractions measurements is checked in 12 different data sub-samples and fitting the points with a constant function returns good χ^2/ndf.

5. T-asymmetry measurement

The K^+ decay sample used for the T-asymmetry measurements is the same as for the branching ratio measurements, except that the missing mass condition is replaced with a stronger selection $|m^2_{miss}(Ke3\gamma)| < 5000\ MeV^2/c^4$ since in this case a lower background contamination is preferred to a smaller sensitivity of the branching ratio measurement to the description of kinematic tails. A_ξ is defined as: $A_\xi = A_\xi^{Data} - (A_\xi^{MCreco} - A_\xi^{MCgene}) \simeq A_\xi^{Data} - A_\xi^{MCreco}$ and a raw measurement of the asymmetry A_ξ is obtained by applying the formula directly to the selected data sample. It is then corrected for the offset introduced by the selection, that is measured with the signal MC sample, by comparing the generated and the reconstructed values of the asymmetry e.g. $A_\xi^{Offset} = A_\xi^{MCreco} - A_\xi^{MCgene}$. But by definition $A_\xi^{MCgene} = 0$ and the final measurement is therefore obtained as $A_\xi = A_\xi^{Data} - A_\xi^{Offset}$. The preliminary results of the measurements of A_ξ, for the three different kinematic ranges, are reported in Table 5.

The A_ξ measurements are actually only an upper limit and their precision is still two orders of magnitude from the theoretical expectation[1, 3, 5, 8]. We can compare our results to the ISTRA+

Table 5: The error budget of the measurements, with the statistical contribution and the different systematic contributions. The total systematic uncertainty is larger than the statistical one, up to a factor of 2. The R_j measurement relative precision is better than 1%.

	R_1 *selection*	R_2 *selection*	R_3 *selection*
$A_\xi = A_\xi^{Data}(\cdot 10^2)$	0.2 ± 0.3	0.1 ± 0.4	-0.6 ± 0.5
$A_\xi = A_\xi^{MCgene}(\cdot 10^2)$	-0.01 ± 0.01	0.00 ± 0.02	-0.01 ± 0.02
$A_\xi = A_\xi^{MCreco}(\cdot 10^2)$	0.3 ± 0.2	0.4 ± 0.3	0.3 ± 0.5
$A_\xi(\cdot 10^2)$	$-0.1 \pm 0.3_{stat} \pm 0.2_{MC}$	$-0.3 \pm 0.4_{stat} \pm 0.3_{MC}$	$-0.9 \pm 0.5_{stat} \pm 0.4_{MC}$

experiment result obtained for the kinematic range R_3: $A_\xi^{ISTRA+}(R_3) = (1.5 \pm 2.1)10^{-2}$. The NA62 measurement in the kinematic range R_3 improves the experimental state of the art by a factor greater than 3 in terms of precision while the two other measurements represent the first ever performed for R_1 and R_2 T-asymmetry.

6. Conclusions

New preliminary results from the NA62 experiment, based on the large $K^+ \to \pi^0 e^+ \nu\gamma$ data sample collected in 2017 and 2018, have been presented.

The experimental relative uncertainties on the measurement of the branching ratio R_j, for 3 kinematic cuts j, are le less than 1%, improving by a factor between 2.0 and 3.6 on the previous measurements. In particular the statistical uncertainty is improved by a factor 3, while the systematic uncertainty is improved by a factor between 2 and 3. The measurements show a 6-7% relative discrepancy with ChPT $O(p^6)$ calculations [3]. The NA62 measurement lies between the most recent theoretical calculations for R_2 [6]. T-asymmetry has been measured for the first time for the R_1 and R_2 kinematic ranges, with an improvement by a factor greater than 3 for the range R_3 with respect to previous measurements.

The T-asymmetry measurement is compatible with zero within the experimental sensitivity, but only imposes a limit two orders of magnitude above the theoretical expectations.

References

[1] J. Bijnens *et al.*, Nucl. Phys. B **396** (1993), 81.

[2] V. V. Braguta *et al.*, Phys. Rev. D **65** (2002), 054038.

[3] B. Kubis *et al.*, Eur. Phys. J. C **50** (2007), 557.

[4] S.A. Akimenko *et al.*, Phys. Atom. Nucl. **70** (2007), 702.

[5] A. Yu. Polyarush *et al.*, Eur. Phys.J. C **81** (2021), 161.

[6] I.B. Khriplovich and A.S. Rudenko, Phys. Atom. Nucl. **74** (2011), 1214.

[7] E. Cortina Gil *et al.*, (NA62 Collaboration), JINST **12** (2017) P05025.

[8] V. V. Braguta *et al.*, Phys. Rev. D **68** (2003), 094008.